# AC and DC Applications of Three-Dimensional Nano-electro-Mechanical-Systems

Anupama B. Kaul[*], Abdur R. Khan[*,**], Krikor Megerian[*], Leif Bagge[*,***]
Larry Epp[*], and Mehmet R. Dokmeci[****]

[*]Jet Propulsion Laboratory, California Institute of Technology, Pasadena, California 91109
[**]Keck School of Medicine, University of Southern California, Los Angeles, CA 90089
[***]Department of Electrical and Computer Engineering, University of Texas, Austin, TX 78712
[****]Department of Electrical and Computer Engineering, Northeastern University, Boston, MA 02115

## ABSTRACT

In this paper, we describe the implementation of carbon nanofibers (CNFs), synthesized using dc plasma enhanced chemical vapor deposition (PECVD), to three-dimensional (3D) dc nanorelays as well as to AC resonator applications. Such nano-electro-mechanical (NEM) structures are under consideration for NASA's extreme environment electronics applications and the 3D architecture promises to increase integration densities by 10X compared to two-dimensional (2D) planar NEMS. Here we describe the fabrication, electrical characterization and modeling results of these vertically oriented CNFs for such 3D NEMS applications.

***Keywords***: carbon nanomaterials, CNFs, nanoelectronics, NEMs, resonators, nanorelays.

## 1 INTRODUCTION

In order to overcome the limitations of solid-state transistors as a result of shrinking device dimensions, nano-electro-mechanical-systems (NEMS) are gaining increasing attention due to their potential for low-power, high-speed and low-leakage current operation. In particular, nanotube-based NEM switches have already been demonstrated for a variety of applications [1,2,3,4], where the tubes were oriented parallel to the substrate. In this paper, we present an architecture where the tubes are oriented perpendicular to the substrate, which has the potential to increase integration densities by 10X compared to two-dimensional (2D) planar NEMS for three-dimensional (3D) electronics applications. Switching between vertically oriented tubes arranged in a 3-terminal configuration was recently reported by Jang *et al*. [5]. A key component of our 3D NEMS architecture is a vertically oriented carbon nanofiber (CNF) synthesized using a plasma-enhanced (PE) chemical vapor deposition (CVD). The refractory metallic nitride electrodes used for actuating and electrically probing the individual CNFs are formed using top-down nanofabrication techniques, prior to the growth of the CNFs. We will describe the fabrication and electrical characterization of the 3D NEMS switches with monolithically integrated electrodes [6], and compare the results to measurements made using nanomanipulation [7].

The AC applications of the 3D NEMS structures are also described here, specifically resonators, which are of interest for communications and mass-sensing applications. The resonators were modeled using a commercially available finite-element-simulator, where the electro-mechanical coupling of the CNF was examined as a function of an incoming AC signal on a probe in close proximity to the tube [8]. These results show that the mechanical resonance was maximized when the frequency of the input signal was equal to the first order harmonic of the CNF. An investigation of the resonance frequency was also performed for various geometrical parameters of our 3D NEMS architecture. *In situ* observations of mechanical resonance in single, vertically oriented tubes was also observed, where such measurements were conducted inside a scanning-electron-microscope (SEM). Nano-mechanical bending tests on individual CNFs were also conducted with the aid of a nanoprobe inside an SEM. Such tests showed the CNF sustained large bending angles ($\phi \sim 70^{o}$) and returned elastically to its initial position without detachment from the substrate or fracture within the tube body.

## 2 DC APPLICATIONS

In Section 2.1 and 2.2, we describe the fabrication and electrical characterization of the 3D NEMS switches, respectively. In Section 2.3, the results of nanomanipulation measurements on the CNFs conducted with a nanoprobe inside an SEM will then be discussed.

### 2.1 Device Fabrication

We have applied top-down nanofabrication techniques to form our 3D NEMS architecture with monolithically integrated electrodes. We initiated the growth of single, vertically aligned tubes using dc PECVD, where a deep UV ($\lambda$ = 248 nm) eximer laser lithography tool (Canon FPA-3000 EX3 stepper) was used in conjunction with chemically

amplified polyhydroxystyrene resin-based deep UV resists to pattern Ni catalyst dots in the few hundred nm diameter range. A positive tone, chemically amplified resist, AZ 8250, was used to define the electrodes, but maintaining a vertical etch profile with minimal undercut of such high aspect ratio nanoscale features required substantial optimization of etch chemistries. As an example, an unoptimized etch chemistry is shown in Fig. 1a, where severe undercut causes the nanoelectrodes to vanish using an inductively coupled plasma (ICP) etcher. In contrast, high aspect ratio nanoscale electrodes with smooth sidewalls are depicted in Fig. 1b, with an optimized etch chemistry using top-down, low-cost, wafer-scale approaches.

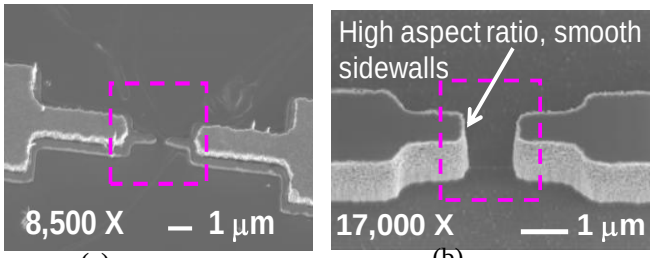


(a) (b)

Figure 1. (a) An unoptimized etch chemistry results in severe undercutting of the nanoelectrodes. (b) Top-down nanofabrication techniques were implemented that yielded high-aspect ratio, nanoscale electrodes with smooth sidewalls using low-cost, wafer scale approaches.

The vertically oriented CNFs were synthesized with pre-patterned Ni catalyst islands. High purity acetylene ($C_2H_2$) and ammonia ($NH_3$) were introduced at 700 ºC, which served as the carbon feedstock and diluent gas, respectively, for the bottom-up synthesis of the CNFs using dc PECVD. When the desired growth pressure had been attained (~ 5 Torr), the dc discharge was ignited at a power of ~ 200 W, and growth was carried out for a fixed duration.

## 2.2 Electrical Characterization

Shown in Fig. 2a is a completed device, where a single vertically oriented CNF is touching an adjacent metal electrode. When a voltage is applied between the electrode and the substrate, currents propagate through the CNF, as the I-V characteristic in Fig. 2b depicts. As higher and higher currents compliances are set, more current propagates through the CNFs. However, increasing the current compliance excessively, for example on Cycle 7 where the compliance was set to ~ 350 nA, we see evidence for damage in the CNF, since on the subsequent cycle, a lower level of current was able to propagate through the CNF. Finally, on cycle 9, no currents are detected for voltages up to 10 V. At this point, inspection of the device in the SEM reveals that the CNF is no longer physically connected to the substrate; the excessive currents have induced damage and caused the CNF to burn and fracture within its body. Shown in Fig. 3 is a switching characteristic of a single CNF where the switching voltage was on the order of ~ 12 volts; the abruptness of the turn-on transition is suggestive of ultra-high switching speeds.

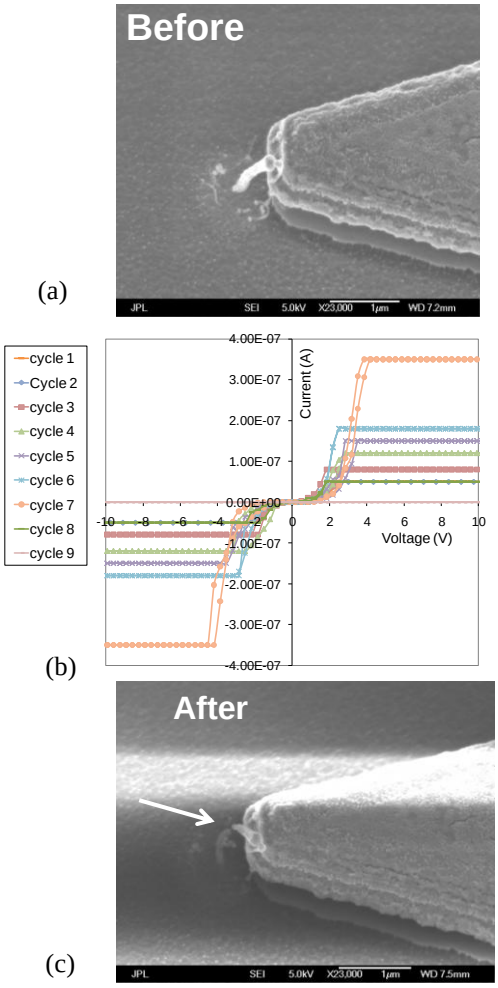


Figure 2. (a) A single CNF that is touching a nanoelectrode on the right. (b) When voltage is applied between the electrode and the substrate, it causes currents to propagate through the CNF as depicted by the I-V characteristic for increasing current compliance levels. (c) The same CNF after excessive currents have been applied to it (e.g. on Cycle 7) that induce damage, causing it to burn and eventually fracture within the body. Cycle 9 shows no current transport up to 10 V, as confirmed by the SEM.

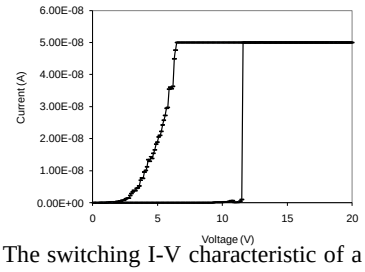


Figure 3. The switching I-V characteristic of a 3D NEMS switch with the monolithically integrated electrodes. Turn-on voltage ~ 12 V where the abruptness of the turn-on transition is suggestive of ultra-high switching speeds.

## 2.3 Nanomanipulation Measurements

*In-situ* measurements have also been conducted on individual, as grown CNFs using a nanomanipulator probe stage (Kammrath and Weiss) mounted inside an SEM. Tungsten probes were used to make 2-terminal contacts, where the substrate served as the ground. The other nanoprobe was mechanically manipulated as depicted in the inset of Fig. 4, so that the nanoprobe is touching a single tube.

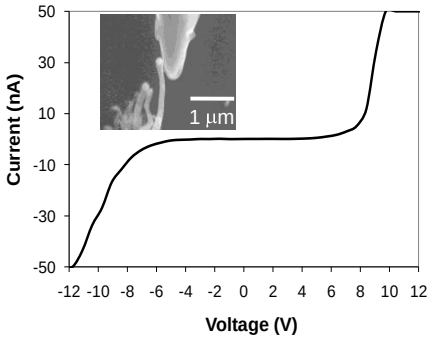


Figure 4. A single CNF that is contacted with a nanoprobe inside an SEM. Electrical measurements show that the CNFs are electrically conductive but there is a large suppressed conductance region for low voltages which may arise from the presence of a native oxide on the probe tips.

We see that while the CNFs are electrically conductive, there is a suppressed conductance region for low voltages where turn-on currents are observed for voltages in excess of ~7-8 V. In contrast, the as-fabricated devices with the monolithically integrated electrodes, we see that the suppressed conductance region in lower, on the order of ~ 2-3V as indicated in Fig. 2b. This may have to do with the presence of a native oxide on the tungsten probe tips. Besides continuity measurements, we have also demonstrated electrostatic switching in the CNFs with the aid or a nanoprobe in an SEM [6].

# 3 AC APPLICATIONS

We have also extended our work on the dc nanoswitches to AC applications, specifically mechanical resonators which have utility in mass sensing as well as communications applications. In Section 3.1, we describe our AC modeling results of our vertically oriented CNFs for 3D NEMS applications, followed in Section 3.2, with empirical results that depict mechanical resonances in the CNF inside an SEM. Finally, in Section 3.3, the results of nanomechanical bending tests on single CNFs is described that shed insight into the mechanical properties of the CNFs.

## 3.1 Resonator Device Modeling

An AC model was developed using COMSOL Multiphysics, which is a commercially available finite-element-simulator [9]. The electro-mechanical coupling of the CNT was examined as a function of an incoming AC signal on a probe in close proximity to the tube. All simulations were performed in a 2D geometry to minimize computational complexity. The CNT was assumed to have a uniform density $\rho \sim 1.5$ g/cm$^3$, elastic modulus $E_b \sim 600$ GPa, relative permittivity $\varepsilon_r \sim 5.0$, and Poisson's ratio, $v \sim 0.2$. Electrostatic boundary conditions were chosen such that the CNT was electrically grounded, and an AC voltage was applied to the adjacent probe. All other boundaries and surfaces were assumed to have zero net electrical charge which is also illustrated by the boundary conditions shown in the schematic of Fig. 5.

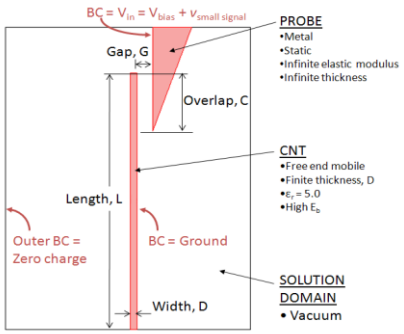


Figure 5. The model geometry for the AC resonator calculations indicating the various boundary conditions used in COMSOL multiphysics.

The modeling results confirmed that the mechanical resonance was maximized when the frequency of the input signal was equal to the first order harmonic of the CNT. An investigation of the resonance frequency was also performed for various geometrical parameters of our 3D NEMS architecture. As an example, the variation of the resonance amplitude with probe-to-tube gap *g* and probe-to-tube coupling length *c* is shown in Fig. 6, where the results appear to confirm expectations. For example, the inset in Fig. 6a shows the amplitude as a function of the frequency for two coupling lengths, and confirms the Q is higher for the larger coupling length of 2000 nm than the 300 nm case.

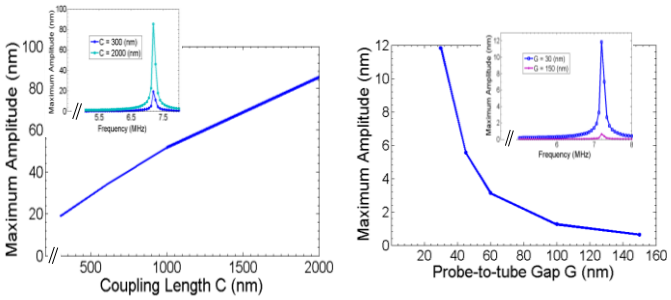


Figure 6. The amplitude of the vibration as a function of the a) coupling length *c* and (b) the gap *g*.

Similarly, Fig. 6b indicates that as the probe is moved further away from the tube, the vibration amplitude

decreases. We note that in Fig. 6b, a $1/g^2$ trend of the deflection amplitude is seen as a function of $g$. The inset in Fig. 6b indicates that the smaller $g$ ~ 30 nm yields a higher Q than a $g$ ~ 150 nm, as expected.

### 3.2 *In situ* Observations of Resonance

Empirical evidence for resonance occurring in the CNFs was also observed from measurements performed *in situ* inside an SEM. Figure 7 shows a large amplitude deflection in an individual, vertically oriented tube as it couples to the nanoprobe, where the deflection was several times the tube diameter.

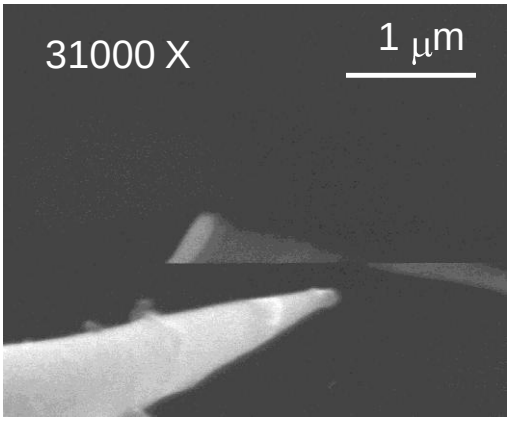


Figure 7. A high amplitude mechanical vibration or resonance observed in a single CNF as it couples to the nanoprobe inside an SEM.

### 3.3 Mechanical Properties

Bending tests were also conducted on individual CNFs using a nanoprobe inside an SEM. The nanoprobe was mechanically manipulated so that it physically deflected the CNF to the right, as shown in Fig. 8a. The CNF sustained bending angles $\phi$ as large as $\phi$ ~ 70º (Fig. 8b), and it then returned elastically to its initial position (Fig. 8c). The CNFs were able to tolerate such severe strains over tens of cycles without detachment from the substrate or fracture within the tube body.

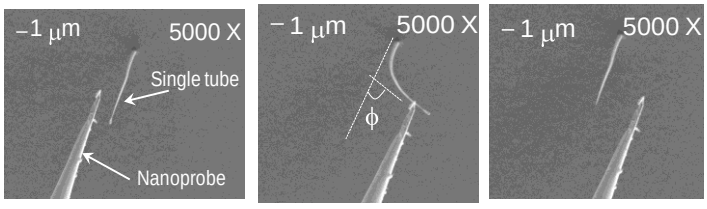


(a) (b) (c)

Figure 8. (a) Bending test on a single CNF with a nanoprobe reveal that the CNF is extremely resilient and able to tolerate bending angles $\phi$ as large as 70º as shown in (b). The CNF returns elastically to its initial position as shown in (c).

These empirical tests show the CNFs are well adhered to the substrate, and demonstrate the exceptional elasticity and resilience of the PECVD synthesized CNFs for both dc and AC NEMS applications, such as nanorelays and resonators, respectively.

## 4 ACKNOWLDEGEMENTS

We would like to thank Robert Kowalczyk, Choonsup Lee for technical assistance and discussions. This research was carried out at the Jet Propulsion Laboratory, California Institute of Technology, under a contract with the National Aeronautics and Space Administration and was funded through the internal Research and Technology Development (R&TD) program.

## REFERENCES

[1] T. Rueckes, K. Kim, E. Joselevich, G. Y. Tseng, C. L. Cheung, and C. M. Lieber, *Science* **289**, 94 (2000).

[2] E. Dujardin, V. Derycke, M. F. Goffman, R. Lefevre, and J. P. Bourgoin, *Appl. Phys. Lett.* **87,** 193107-1 (2005).

[3] A. Eriksson, S. Lee, A. Sourab, A. Issacsson, R. Kaunisto, J. M. Kinaret, and E. E. B. Campbell, *Nano Lett.* **8**, 1224 (2008).

[4] A. B. Kaul, E. W. Wong, L. Epp, and B. D. Hunt, *Nano Lett.* **6**, 942 (2006).

[5] J. E. Jang, S. N. Cha, Y. Choi, G. A. J. Amaratunga, D. J. Kang, D. G. Hasko, J. E. Jung, and J. M. Kim, *Appl. Phys. Lett.* **87**, 163114 (2005).

[6] A. B. Kaul, K. Megerian, and A. R. Khan, "A 3D NEMS switch with monolithically integrated electrodes," submitted (in review).

[7] A. B. Kaul, A. Khan, L. Bagge, K. G. Megerian, H. G. LeDuc, and L. Epp, *Appl. Phys. Lett.* 95, 093103 (2009). Also selected for the *Virtual Journal of Nanoscale Science & Technology*, Sep. 14 (2009).

[8] L. Bagge, L. Epp, A. Khan, and A. B. Kaul, *J. Nanosci. and Nanotechnol.* 10, 6388 (2010).

[9] COMSOL Multiphysics Version 3.4, COMSOL AB, Tegnérgatan 23, SE-111 40, Stockholm, Sweden. www.comsol.com.